Mater. Res. Soc. Symp. Proc. Vol. 1157 © 2009 Materials Research Society 1157-E06-02

Fundamental Mechanisms of Copper CMP – Passivation Kinetics of Copper in CMP Slurry Constituents

Shantanu Tripathi[1], Fiona M. Doyle[2], and David A. Dornfeld[1]
[1]Department of Mechanical Engineering, University of California,
Berkeley, CA 94720-1740, U.S.A.
[2]Department of Materials Science and Engineering, University of California,
Berkeley, CA 94720-1760, U.S.A.

ABSTRACT

During copper CMP, abrasives and asperities interact with the copper at the nano-scale, partially removing protective films. The local Cu oxidation rate increases, then decays with time as the protective film reforms. In order to estimate the copper removal rate and other Cu-CMP output parameters with a mechanistic model, the passivation kinetics of Cu, i.e. the decay of the oxidation current with time after an abrasive/copper interaction, are needed. For the first time in studying Cu-CMP, microelectrodes were used to reduce interference from capacitive charging, IR drops and low diffusion limited currents, problems typical with traditional macroelectrodes. Electrochemical impedance spectroscopy (EIS) was used to obtain the equivalent circuit elements associated with different electrochemical phenomena (capacitive, kinetics, diffusion etc.) at different polarization potentials. These circuit elements were used to interpret potential-step chronoamperometry results in inhibiting and passivating solutions, notably to distinguish between capacitive charging and Faradaic currents.

Chronoamperometry of Cu in acidic aqueous glycine solution containing the corrosion inhibitor benzotriazole (BTA) displayed a very consistent current decay behavior at all potentials, indicating that the rate of current decay was controlled by diffusion of BTA to the surface. In basic aqueous glycine solution, Cu (which undergoes passivation by a mechanism similar to that operating in weakly acidic hydrogen peroxide slurries) displayed similar chronoamperometric behavior for the first second or so at all anodic potentials. Thereafter, the current densities at active potentials settled to values around those expected from polarization curves, whereas the current densities at passive potentials continued to decline. Oxidized Cu species typically formed at 'active' potentials were found to cause significant current decay at active potentials and at passive potentials before more protective passive films form. This was established from galvanostatic experiments.

INTRODUCTION

We are developing a mechanistically-based tribo-chemical model for copper CMP that treats the bulk of the material removal as wear-enhanced corrosion. The model considers a copper surface to be protected by inhibitor or a protective film, depending upon the chemical nature of the slurry. The protective film is periodically removed, at least partially, by interaction with pad asperities and abrasive particles in the slurry. The corrosion current increases, then decays as the protective film builds up again until the next abrasive event. Information in the literature [1] suggests that the frequency of interactions of pad asperities with a given site on copper, τ, is about every ms.

Let *i(t')* be the transient passive current density at time *t'* after bare copper is exposed to a given oxidizing passivating environment, and i_0 be the current density immediately after an abrasive-copper interaction (which would only be *i(t')* if the interaction removed the entire film). If *t* is the time since the last abrasive-copper interaction, with t_0 defined such that $i(t'=t_0)=i_0$, then the average removal rate of copper between the two abrasive-copper interactions is:

$$\dot{V}_{CW} = \frac{M_{Cu}}{\rho n F \tau} \int_0^{\tau} i(t_0 + t)dt \qquad (1)$$

where M_{Cu} is the atomic mass of copper, ρ is the density of copper, *n* is the oxidation state of the oxidized copper, and *F* is Faraday's constant. In order to evaluate the integral, and hence to calculate the removal rate of copper, it is necessary to know the rate at which the current decreases with time. This is challenging, experimentally, because the time scale of interest is very short, on the order of ms.

Two different techniques were examined for studying copper passivation kinetics immediately after creating bare copper. The first was scratch-repassivation, whereby a copper rod is held at the potential of interest in an appropriate solution, and rotated against a sharp tool to scratch through any passive film that may be present. The current is monitored before, during and after scratching; the decay current provides the kinetics of repassivation. Unfortunately, this technique introduces more surface damage than would be expected during CMP, and hence the passivation current would be expected to be unrealistically high. Experimentally, we found that vibrations and instabilities caused significant noise, along with currents that tended to drift higher while scratching because of an increasing scratch size. Hence, we focused on the second technique, potential-step chronoamperometry. In this technique, the copper is initially held at a low potential, to allow cathodic reduction of any oxidized species that may be present on the surface. The potential is then stepped up to the anodic potential of interest, and the resulting current is monitored. When passivation occurs, or inhibitor is adsorbed onto the surface, the current decreases. Challenges in interpreting the response from potential-step chronoamperometry include Ohmic drops across the solution, the fact that the measured current includes capacitive charging in addition to the Faradaic current, diffusion that may change the composition at the copper-electrolyte interface, and rapidly changing currents that may cause potential oscillations. These effects can be reduced by using a microelectrode; the small currents minimize the Ohmic drops, and there is faster charging and diffusion. Furthermore, a microelectrode better simulates the scale of copper features during CMP than a macroelectrode.

EXPERIMENTAL PROCEDURE

Electrochemical experiments were conducted using a Gamry Series G 300 Potentiostat. The microelectrode used was a 34 gauge (80µm radius) copper wire (99.95% purity, MWS Wire Industries) insulated by enamel coating, with the exposed end acting as the microelectrode. A fresh copper surface was exposed by cutting off the end of the wire with a fine blade before each set of experiments. Before each experiment, the microelectrode was conditioned at a cathodic potential between -1.5 and -1V for 30s to remove any oxidized surface species or films.

Three different electrolytes were used: a pH 12 electrolyte containing 0.01M glycine (>99% from Acros Organics Co.) with pH controlled using NaOH (reagent grade from Fisher Scientific

Co.); a pH 4 solution buffered using acetic acid/sodium acetate with 0.01M glycine; and a similar solution also containing 0.01M benzotriazole (BTA) (from Aldrich Chemical Co.). All solutions were prepared using deionized water at 24°C. All experiments used 500 mL electrolyte

A three-electrode electrochemical cell, housed in a glass cylinder 130 mm high, with a 120 mm interior diameter, was used for all experiments. The microelectrode was suspended at the center of the cell. A saturated calomel reference electrode (SCE) [0.242 V vs the standard hydrogen electrode (SHE)] was placed 1 cm away from the wall of the cell. A platinum mesh counter electrode was held 1 cm from the wall of the cell diametrically opposite to the reference electrode. All potentials are reported with respect to the SCE. DC potentiodynamic polarization experiments were conducted from about -1V below the open circuit potential (E_{OC}) to about 1.5V above E_{OC}. Electrochemical impedance spectroscopy (EIS) was conducted at different DC potentials after holding copper at the particular DC potential for 60s, using an AC voltage amplitude of 10mV (rms). The frequency was varied from 300kHz to 0.1Hz, with 10 points per frequency decade. Chronoamperometry tests were conducted by stepping from one potential to another and recording the current densities over time at the new potential. The initial voltage, the time at initial voltage, and the final voltage were varied to examine the passivation kinetics.

RESULTS

Figures 1 and 2 show potentiodynamic polarization curves measured in pH 4 and 12 solutions containing 0.01 M glycine. At pH 4 there was active corrosion at all anodic potentials, whereas at pH 12 there was pronounced passivation between about 0 V and 0.8 V SCE. EIS measurements were taken at the potentials indicated by the arrows in these curves, and fitted to equivalent circuits to obtain equivalent electrical parameters for the different conditions.

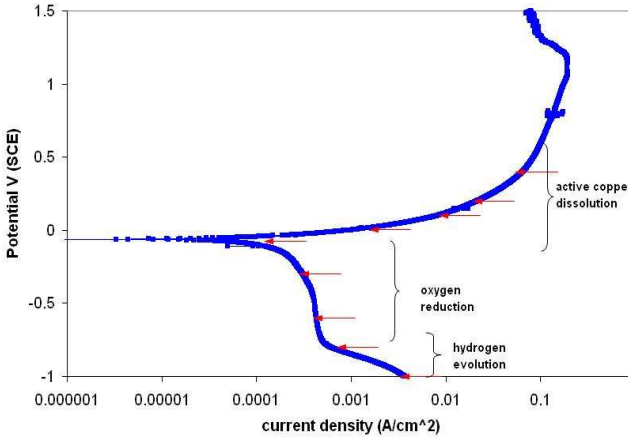

Figure 1: Potentiodynamic polarization curve (10mV/s) of a copper microelectrode in pH 4 aqueous solution with 0.01M glycine. EIS was conducted at potentials indicated by arrows

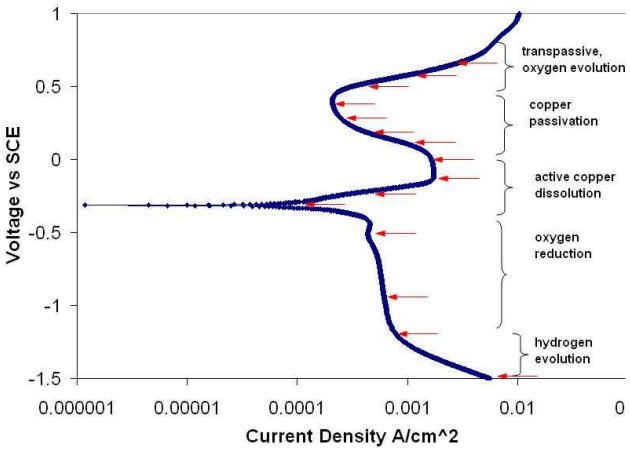

Figure 2: Potentiodynamic polarization curve (10mV/s) of a copper microelectrode in pH 12 aqueous solution with 0.01M glycine. EIS was conducted at potentials indicated by arrows

Chronoamperometry at pH 4

Knowing the equivalent electrical parameters for the different conditions allows evaluation of the capacitive charging and diffusion-limited currents in a given experiment. This then allows discernment of the Faradaic portion of the current; only this provides the passivation kinetics. To assess the quality of the electrical parameters obtained from the EIS studies, they were used to simulate potential-step chronoamperometric behavior in pH 4 aqueous glycine with no BTA, where no passivation is expected. The maximum predicted R_UC_{DL} is around 3 ms, hence capacitive charging should be over by about 15 ms (5* R_UC_{DL}). Figure 3 shows the current predicted after stepping to 0.1V from different potentials, while Figure 4 shows experimental data for stepping to 0.2V; both final potentials were anodic, as seen in Figure 1. It is seen that by about 10 – 15 ms, the currents have settled to a steady, almost constant value; along with the good agreement between the predicted and experimental data, this demonstrates the reliability of the fitted electrical parameters.

Figure 5 shows the experimental current decay after stepping up to different potentials from -1.2V (SCE) in pH 4 aqueous glycine containing BTA. The decay behavior is very similar for all potentials. The capacitive charging is predicted to be over in less than a millisecond (EIS data show the maximum R_UC_{DL} to be 0.3ms). For potentials from -0.2V to 0.4V the current decays steadily at 0.5 orders of magnitude per time decade from about 1 ms, i.e. the current density varies as the inverse of the square root of time. This suggests a Cottrell type decay behavior i.e. the current densities are diffusion limited. The behavior is very different from that in the absence of BTA[2], suggesting that diffusion of BTA to the surface is controlling the rate of inhibition. At some of the higher potentials (>0.4V), current densities stop dropping after 1s, probably because a monolayer of BTA has formed. At lower potentials (< -0.2V), the anodic currents continue to decline over time, suggesting that thick layers of BTA are forming. At these lower potentials, the cathodic reaction (hydrogen evolution) eventually becomes larger in magnitude than the diminishing anodic reaction, causing the overall current to become cathodic.

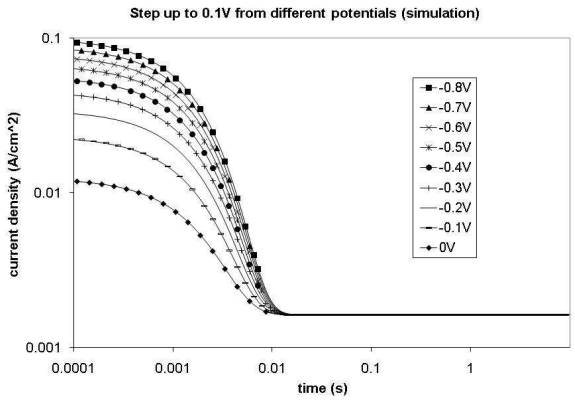

Figure 3: Simulation of current decay after stepping up from different initial potentials to fixed final potential (0.1V) for a Randles cell with electrical parameters relevant to pH 4

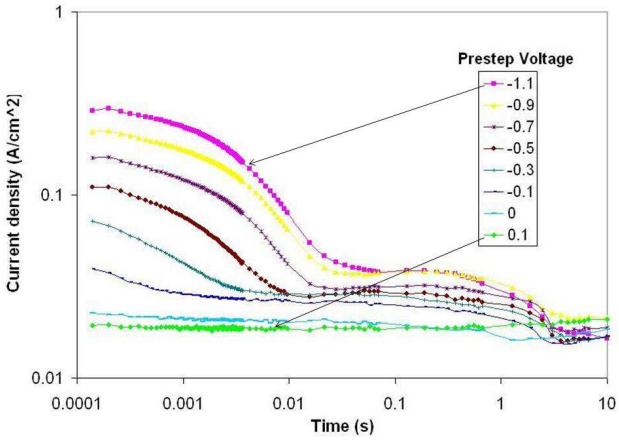

Figure 4: Current decay after stepping from different potentials (held for 10s) to 0.2V (fixed range data acquisition), copper in pH 4 aqueous solution containing 0.01M glycine

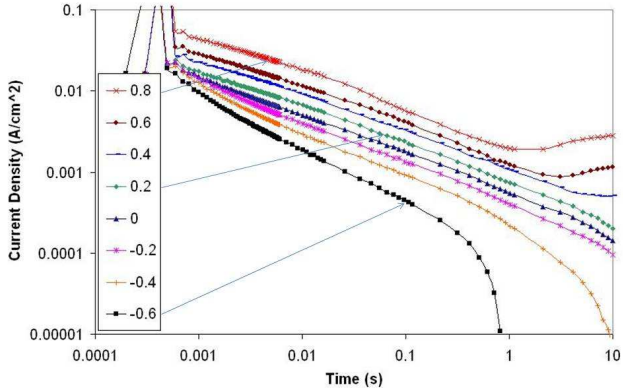

Figure 5: Current decay on copper after stepping potential from -1.2V to different potentials, copper in pH 4 aqueous solution containing 0.01M glycine and 0.01M BTA

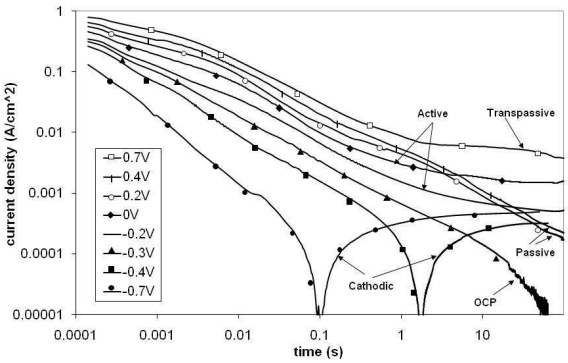

Figure 6: Current decay after stepping from -1V to different potentials (composite data from different data acquisition modes, with data smoothing filters applied): copper in pH 12 aqueous solution containing 0.01M glycine

Chronoamperometry at pH 12

Figure 6 shows the current decay at pH 12 after stepping from -1.0V to potentials in the active, passive, transpassive and cathodic regions (although pH 12 slurries are not used in CMP, the surface pH is high when H_2O_2 is used as an oxidizing agent, so these conditions represent weakly acidic slurries containing H_2O_2). For the first second or so, the current decay at all potentials above E_{OC} is very similar, dropping by about 2 orders of magnitude from the peak current densities. After about 1 s the current densities for active or transpassive potentials settled close to the values expected from Figure 2, whereas for the passive potentials the current densities continued to drop steadily. The maximum R_UC_{DL} value expected from EIS data is 0.8ms, so capacitive charging should be completely over by about 4ms (= 5*R_UC_{DL}). Thereafter, the current should have settled to the final Faradaic value. Figure 7 confirms this; the current passing at 0.1 ms is linearly dependent on the potential step, demonstrating that it is capacitive

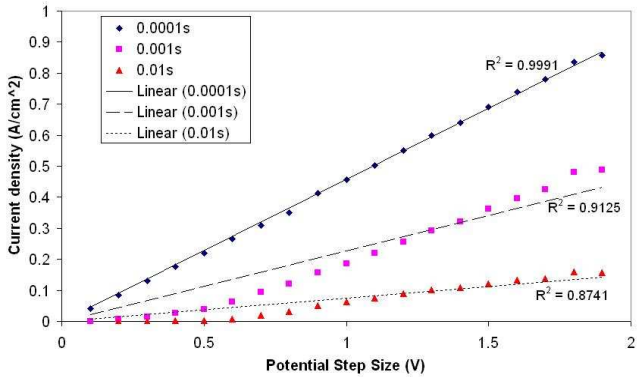

Figure 7: Current densities vs. potential step at different times after the potential step (step up from -1V to different potentials): copper in pH 12 aqueous solution containing 0.01M glycine

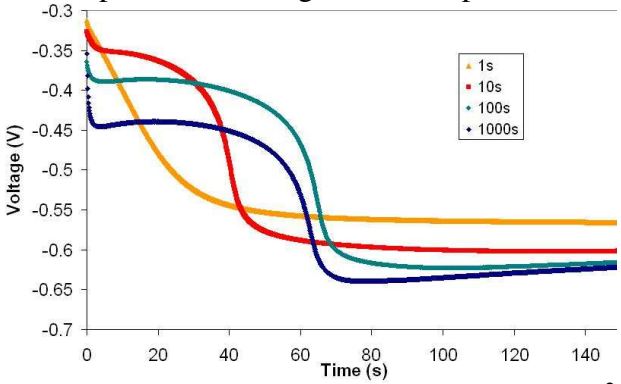

Figure 8: Galvanostatic reduction at -0.1mA/cm^2 after polarizing at a passive potential (0.2V SCE) for different times (see legend), copper working electrode in pH 12 aqueous solution containing 0.01M glycine and 10^{-4}M $CuNO_3$.

charging. At 1ms and 10ms, the relationship is no longer linear, showing that Faradaic current predominates.

The similarity in current decay between 1 ms and 1 s is interesting, in that it is seen at potentials at which copper dissolves actively and potentials where copper is passivated. Hence this behavior cannot be due to protective oxide films. Figures 8 shows galvanostatic reduction curves obtained at pH 12 on a macroelectrode that had been held at a passive potential (0.2V) for different time periods, before passing a constant reduction current of -0.1 mA/cm^2. After passivation for 10, 100 or 1000 s, the potentials dropped initially, then stayed nearly constant while the passive layers were reduced. The potential then dropped further, and hydrogen was discharged. The reduction potential of the layers decreased with increasing formation time, suggesting that the oxide stabilizes with time, requiring a higher overpotential for reduction. The layer formed over 10 s was fully reduced within 40 s, while those formed over 100 and 1000 s required longer, indicating that they were thicker. In contrast, the potential of the sample that was held at 0.2V for only 1 s dropped steadily, suggesting that there was no passive layer (instead, reduction probably involved reduction of Cu(II) ions being transported back to the electrode from the solution). This is consistent with the conclusion above that protective oxide films do not form in the first second. Instead, the decrease in current must be due to adsorption of oxidized species onto the copper. This conclusion is extremely significant for copper CMP modeling. Given the short time interval between interactions of pad asperities or abrasive particles with a given site on the copper surface (typically around 1 ms), there is not time for coherent oxide layers to develop. Hence copper CMP is best considered to be plucking of oxidized species from a film of adsorbed species, rather than as mechanical abrasion of a coherent oxidized layer.

CONCLUSIONS

Potential step chronoamperometry was used to measure the passivation kinetics of copper over very short time periods. EIS data were successfully applied to distinguish capacitive charging from the Faradaic currents relevant to material removal in CMP. Although the behavior differed in aqueous glycine solutions at pH 4 with BTA and at pH 12, in both cases the Faradaic current decreased at a well defined rate that could be incorporated into a CMP model.

ACKNOWLEDGMENTS

This work was funded by AMD, Applied Materials, ASML, Cadence, Canon, Ebara, Hitachi, IBM, Intel, KLA-Tencor, Magma, Marvell, Mentor Graphics, Novellus, Panoramic, SanDisk, Spansion, Synopsys, Tokyo Electron Limited, and Xilinx, with donations from Photronics, Toppan, and matching support by the U.C. Discovery Program.

REFERENCES

1. C.L. Elmufdi, G.P. Muldowney, “A Novel Optical Technique to Measure Pad-Wafer Contact Area in Chemical Mechanical Planarization” Mater. Res. Soc. Symp. Proc. V91, 2006 Spring
2. S. Tripathi, “Tribochemical Mechanisms of Copper Chemical Mechanical Planarization (CMP) – Fundamental Investigations and Integrated Modeling”, Ph.D. Dissertation, University of California, Berkeley, December 2008.